

Topmost layer magnetization of ultrathin Cr films on Fe(100) from proton-induced spin-polarized electron emission

R. Pfandzelter,* M. Ostwald, and H. Winter

Humboldt-Universität zu Berlin, Institut für Physik, Invalidenstrasse 110, D-10115 Berlin, Germany

(Received 24 January 2001; published 16 March 2001)

The magnetic ordering of the topmost surface layer of ultrathin Cr films grown on Fe(100) is studied via spin-polarized electron emission, excited by fast protons grazingly scattered from the film surface. We find that most electrons originate from the topmost layer. Based on simple assumptions we are able to deduce the layer-dependent magnetic moments from the observed spin polarization of electrons. We demonstrate that our method has a clearly smaller probing depth than conventional spin-polarized electron spectroscopies.

DOI: 10.1103/PhysRevB.63.140406

PACS number(s): 75.70.Ak, 79.20.Rf, 79.20.Hx

Fe/Cr/Fe sandwiches and superlattices have evolved into a prototype system to study interlayer exchange coupling and the giant magnetoresistance effect. During recent years, considerable experimental and theoretical work has been performed on these artificially layered magnetic structures leading to outstanding discoveries.¹ The basic building block of these multilayers are bare films of Cr epitaxially grown on Fe(100). In this communication we present studies on the magnetic structure of ultrathin Cr films on Fe(100) using a different technique: spin-polarized emission of electrons induced by grazing proton impact. A striking feature of this technique is the extreme sensitivity to the topmost film layer, in comparison to larger probing depths in conventional electron-induced electron emission spectroscopies.²

Considerable progress has been achieved concerning knowledge of the structural and chemical properties of ultrathin Cr films on Fe(100). Growth is epitaxial and pseudomorphic in a wide range of temperatures.³⁻⁶ Almost perfect layer-by-layer growth is achieved for substrate temperatures around 600 K, whereas lower temperatures lead to kinetic roughening of the film. Recently it has been observed that growth of the first layer leads to the formation of a Cr-Fe alloy,⁷⁻⁹ which is essentially confined to the surface and subsurface layer. For converges of more than two monolayers (ML) the topmost layer consists almost exclusively of Cr atoms.^{8,9}

Most studies have focused on the magnetic properties of the Cr films since the seminal discovery of a layer-by-layer antiferromagnetic ordering in several ML thick Cr films.³ Although a number of experimental techniques, mainly based on spin- and, in some cases, energy-resolved scattering of electrons, have been applied, the magnetic behavior of the first few layers remained unclear. Walker *et al.*¹⁰ infer from slightly negative asymmetries in spin-polarized electron-energy-loss spectroscopy that 1 ML Cr grown at 470 K couples antiferromagnetically to Fe, in agreement with results from magnetically sensitive core level spectroscopies.¹¹⁻¹³ Upon further deposition, the asymmetry maintains the same sign as for clean Fe up to coverages of about 8 ML. A similar behavior is observed using electron-excited spin-polarized electron emission (secondary electron emission spectroscopy) for room temperature growth.¹⁴ After background subtraction, a negative spin polarization is inferred for the 1 ML Cr film. Subsequent layers show a posi-

tive spin polarization which gradually decreases with increasing film thickness. Using the same technique, although without energy resolution, Unguris *et al.*^{3,8} succeeded in observing layer-by-layer oscillations in the spin polarization starting from the fourth layer for growth at 570 K.

A common feature of techniques based on electron-induced electron emission is a signal stemming from a depth region comprising a few layers beneath the surface. Extraction of the overlayer signal thus requires modeling and subtraction of a generally spin- and energy-dependent background.^{2,14} It is evident that this poses problems in cases like Cr on Fe, where interfacial alloying and largely different layer magnetizations are expected (in Refs. 3 and 8 Cr-overlayer induced features in the observed spin polarization amount to only a few percent of the underlying background polarization for the first few layers grown).

In this communication we demonstrate a significant reduction of the probing depth in spin-polarized electron emission spectroscopy by using fast protons instead of electrons as primary particles. The protons are scattered under grazing angles from the surface layer without penetrating into the film ("surface channeling"¹⁵). Thus, in contrast to the almost uniform in-depth generation of secondary electrons by primary electrons, proton-induced electrons originate mainly from the topmost surface layer. Common to both techniques is that the emission results from a transfer of kinetic energy of the primary particle to electrons of the film. In this respect our method differs from related techniques, where the potential energy of impinging ions causes emission or capture of spin-polarized electrons.¹⁶⁻¹⁹

The experiments are performed at a pressure of some 10^{-11} mbar. The Fe crystal is mounted to close the gap of a soft-magnetic yoke with a coil. The crystal is magnetically saturated by current pulses along an easy axis of magnetization [001] or $[00\bar{1}]$ within the (100) surface plane and perpendicular to the scattering plane. With the magneto-optic Kerr effect we find a square-shaped hysteresis loop with full remanence near the center of the target and a reduced remanence near the edges. All data are recorded in the remanent state. The Fe target is prepared by cycles of grazing sputtering with 25 keV Ar⁺ ions and subsequent annealing, until the surface is clean and flat (mean terrace width >1000 Å),

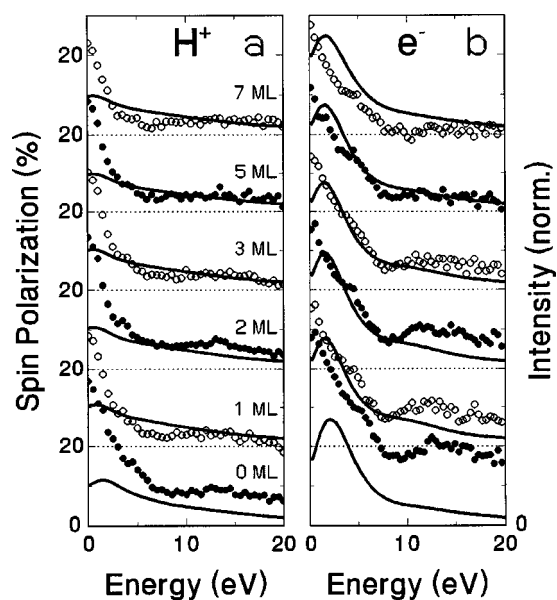


FIG. 1. Normalized intensity distribution (curves, right-hand ordinate) and spin polarization (symbols, left-hand ordinate) of electrons excited by 25 keV H^+ ions (a) and 4 keV electrons (b). The spectra refer to the clean Fe(100) surface (bottom) and Cr coverages (averaged over a coverage range of ± 0.2 ML in each case) as indicated. The polarization is calculated from the measured asymmetry with a Sherman function of 0.2. The origins are displaced vertically by constant amounts (dashed lines).

as checked by low-energy electron diffraction (LEED), Auger spectroscopy, and angular distributions of scattered ions.²⁰

Cr is sublimated by electron beam heating. Growth is monitored *in situ* and in real time by measuring the specular intensity of grazing scattered ions. This technique enables one to calibrate the coverage and quantitatively determine the film morphology. For the present study we choose a growth temperature of about 610 K, where growth is found to proceed in an almost perfect layer-by-layer mode, in accordance with our previous studies.⁶ Typical growth rates are some 10^{-4} ML s^{-1} .

Emitted electrons are collected within a cone of about 12° full opening angle around a direction of 10° off normal and enter a cylindrical sector field energy analyzer via a transfer lens (CSA300, Focus). After energy separation and 90° deflection, electrons are imaged by another lens into a LEED spin-polarization detector.²¹ Pass energy (80 eV), energy resolution [3.0 eV full width at half maximum (FWHM)], and LEED scattering energy (104.5 eV) are kept constant during energy scans. Each polarization spectrum is obtained from two identical measurements with reversed magnetization to eliminate instrumental asymmetries and checked by measurements on a paramagnetic Ta foil attached directly near the Fe sample.

In Fig. 1(a) we show intensity distribution (curves) and spin polarization (symbols) of electrons excited by 25 keV H^+ ions incident at a grazing angle of 1.2° upon the clean and Cr-covered Fe(100) surface. For comparison we also use 4 keV electrons at oblique incidence (33°) as primary par-

ticles (b). The spectra were recorded at 610 K during Cr growth. In order to discriminate secondary electrons generated at surfaces in the chamber other than the target surface, we biased the target by -10 V with respect to ground.²² We estimate an increase of the effective solid angle at small electron energies (electron trajectory calculations show 30% at 5 eV), which at least partly compensates for the energy dependence of the transmission due to residual magnetic stray fields.

The intensity distributions in Fig. 1 (curves) exhibit the well-known behavior: a pronounced peak with a maximum at 1–2 eV and a gradual decrease towards higher energies. The peak is usually ascribed to cascade multiplication owing to kinetic electron-electron collisions, whereas direct excitation of electrons by primary particles should dominate at higher energies. Although details of the intensity distributions will be discussed elsewhere, we would like to mention two observations here: (i) Aside from a shift of the maximum to smaller energies, the effect of the Cr coverage is weak. (ii) The cascade peak is less pronounced for H^+ excitation, but we do not observe significant differences between electron and proton excitation. This is in contrast to Ref. 19, where similar experiments on clean surfaces are interpreted solely in terms of potential emission by ion impact.

The observed spin polarization (Fig. 1, symbols) is in agreement with previous studies on electron-induced electron emission.^{23,24} It is largest for small energies and falls rapidly within the range of cascade electron energies [Fig. 1(b)]. This is also observed for proton excitation [Fig. 1(a)]. This similarity between proton and electron excitation is remarkable, as it shows that cascade effects are important even for grazing angles of incidence. We note that, for the clean Fe surface, the polarization is smaller for proton impact than for electron impact. This can be, at least partly, ascribed to the larger source area (reduced magnetization near the sample edge) and the smaller probing depth (thermally reduced magnetization at the surface).

Although the overall shape of the spin polarization spectra hardly changes upon growth of Cr, we observe for proton excitation a strong and nonmonotonic dependence of the values of the polarization on the coverage. This is in clear contrast to the gradual decrease observed for electron excitation. The effect becomes more evident when the measured spin polarization is averaged over the whole spectral range (excluding small energies $E < 2$ eV) and plotted against the Cr coverage. For proton excitation [Fig. 2(a)] the spin polarization follows a series of roughly linear variations. The breakpoint positions coincide with integer ML coverages. This oscillatory behavior clearly differs from electron excitation [Fig. 2(b)], where, aside from the first layer, the layer-by-layer growth of Cr does not appear in the observed polarization. We note that the shape of the spin polarization curves (Fig. 2) hardly depends on the choice of energy interval for energies larger than a few eV, if normalized to the data for the clean Fe surface.

Considering the conceptual and physical similarity of both experiments, the striking difference between the observed polarization curves may be ascribed to different probing depths for proton and electron excitation, respectively.

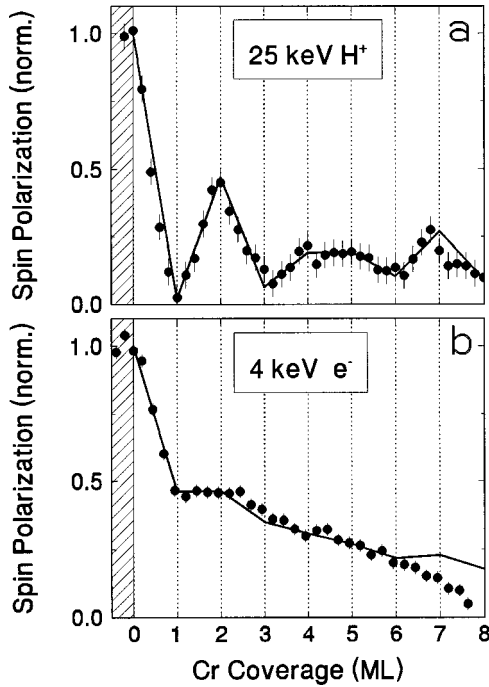


FIG. 2. Spin polarization (symbols) of electrons excited by impact of 25 keV H^+ ions (a) and 4 keV electrons (b) on Cr/Fe(100) versus Cr overlayer thickness. The solid lines represent model calculations assuming the same layer-dependent magnetization profile but different probing depths for proton and electron excitation (see text). The data have been normalized to the polarization for the clean Fe surface.

Whereas grazingly scattered protons mainly excite electrons from the top-most film layer, the probing depth for electron excitation amounts to several layers. An antiferromagnetic stacking of layers, as expected for Cr/Fe(100), thus causes a gradual decrease of the measured polarization with increasing coverage, in agreement with our observation and previous studies on electron-induced electron emission.^{3,14} Nevertheless, we do not observe a layer-by-layer change in sign for proton impact, in agreement with the highly surface sensitive experiments of Walker *et al.*¹⁰

The layer-dependent magnetic moments can be estimated by fitting the data for proton excitation from Fig. 2(a), assuming a proportionality between spin polarization and magnetization,

$$P \propto \frac{\sum_i n_{Ba,i} \exp(-z_i/\lambda_a) + n_{Bs} \lambda_s \exp(-d/\lambda_a)}{\sum_i n_{a,i} \exp(-z_i/\lambda_a) + n_s \lambda_s \exp(-d/\lambda_a)}, \quad (1)$$

where $n_s(n_{a,i})$ is the number of conduction electrons per atom in the substrate (film layer i), $n_{Bs}(n_{Ba,i})$ the Bohr magneton number, d the film thickness, and $\lambda_s(\lambda_a)$ the attenuation length of electrons in the substrate (film). $n_{a,i}$ is slightly layer dependent due to interfacial alloying.^{7,9} We assume $n_{Bs} = 0.9 \times 2.13 = 1.92$ (the prefactor takes account of thermal spin excitations) to be independent on the depth. For a uniform in-depth generation of electrons as in electron excita-

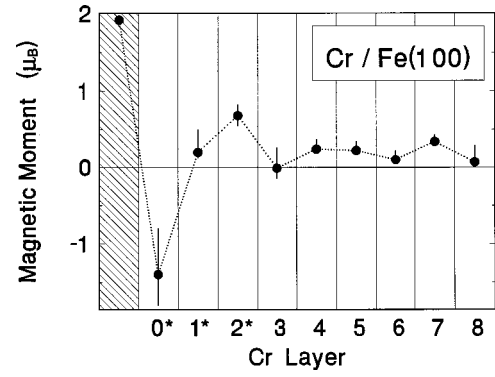


FIG. 3. Layer-dependent magnetic moments per atom for Cr/Fe(100) obtained from a fit to the data from Fig. 2 according to Eq. (1). Layers 0* and 1* (alloyed layers are marked by *) refer to the subsurface and surface layer, respectively, after deposition of 1 ML of Cr. The error bars cover statistical errors and systematic errors due to the choice of electron energy interval and the uncertainty of probing depth.

tion, attenuation lengths have been compiled in Ref. 25. Here $\lambda_s = 4.2$ ML (Fe) and $\lambda_a = 2.9$ ML (Cr) (we neglect the spin dependence observed for the smallest energies $E < 10$ eV). On the other hand, for grazing proton impact, we expect $\lambda \rightarrow 0$. Yet there is a finite probability for the protons to penetrate the surface via ledges of islands, substrate steps, or thermally displaced atoms. From trajectory simulations²⁰ we estimate $\lambda_s = \lambda_a = (0.5 \pm 0.3)$ ML.

The layer-dependent magnetic moments obtained from a fit to the data for proton excitation [Fig. 2(a), solid lines] are shown in Fig. 3. As expected, the plot closely resembles the spin polarization curve. Note, however, that the moments deduced for the alloyed layers 0*, 1*, and 2* represent averaged moments of Fe and Cr atoms. Our results show that there are significant deviations from the layer-by-layer oscillations of Cr moments observed for thicker layers.³ This is most evident for coverages of 1 or 2 ML, where considerable alloying occurs. From the third monolayer, the observed moments are similar to the rms Cr bulk moment (about $0.4 \mu_B$). Aside from the unexpected magnetic ordering at the beginning of growth, our data suggest another irregularity between layers 4 and 5. This would explain the anomalous phase of the magnetic stacking observed in thicker layers.³

Note that an averaged moment of $-1.4 \mu_B$ for the interface layer 0* would imply huge negative moments for Cr atoms ($-4.7 \mu_B$), if we assume Fe moments as in the bulk ($1.92 \mu_B$). Such huge Cr moments ($-4.5 \mu_B$) have been also observed by Turtur and Bayreuther²⁶ during initial growth at room temperature by absolute magnetometry.

With the layer-dependent magnetic moments from Fig. 3, we calculated the spin polarization curve for electron excitation [Fig. 2(b), solid lines], also by using Eq. (1), but with larger attenuation lengths. The consistency of the data sets corroborates our assumption of different probing depths in proton and electron excitation. We note that the reverse procedure (deduction of moments from measured spin polarizations) leads to ambiguous results.

In summary, we studied the magnetic ordering of ultrathin

Cr films on Fe(100) by spin-polarized electron emission. The films were grown under conditions where growth is almost perfectly layer-by-layer and the chemical composition is well known. In addition to conventional excitation by electrons, we used grazing impact of fast protons. The observed spin polarization of emitted electrons shows layer-by-layer oscillations for early Cr growth, in contrast to the gradual decrease observed for excitation by electrons. The extreme sur-

face sensitivity for proton excitation enables one to deduce magnetic moments of the topmost film layer in a straightforward manner.

The assistance of T. Igel, A. Laws, K. Maass, and R. A. Noack in the preparation of the measurements is gratefully acknowledged. This work was supported by the Deutsche Forschungsgemeinschaft (Sonderforschungsbereich 290).

*Email address: pfandz@physik.hu-berlin.de FAX: +49 30 2093 7899.

¹K. B. Hathaway, A. Fert, P. Bruno, D. T. Pierce, J. Unguris, R. J. Celotta, S. S. P. Parkin, in *Ultrathin Magnetic Structures II*, edited by B. Heinrich and J. A. C. Bland (Springer, Berlin, 1994), p. 45, and references therein.

²H. C. Siegmann, *J. Phys.: Condens. Matter* **4**, 8395 (1992).

³J. Unguris, R. J. Celotta, and D. T. Pierce, *Phys. Rev. Lett.* **69**, 1125 (1992); D. T. Pierce, R. J. Celotta, and J. Unguris, *J. Appl. Phys.* **73**, 6201 (1993).

⁴B. Heinrich and J. F. Cochran, *Adv. Phys.* **42**, 523 (1993).

⁵D. T. Pierce, J. A. Strosio, J. Unguris, and R. J. Celotta, *Phys. Rev. B* **49**, 14 564 (1994).

⁶R. Pfandzelter, T. Igel, and H. Winter, *Surf. Sci.* **375**, 13 (1997).

⁷D. Venus and B. Heinrich, *Phys. Rev. B* **53**, R1733 (1996).

⁸A. Davies, J. A. Strosio, D. T. Pierce, and R. J. Celotta, *Phys. Rev. Lett.* **76**, 4175 (1996); A. Davies, J. A. Strosio, D. T. Pierce, J. Unguris, and R. J. Celotta, *J. Magn. Magn. Mater.* **165**, 82 (1997).

⁹R. Pfandzelter, T. Igel, and H. Winter, *Phys. Rev. B* **54**, 4496 (1996); *Surf. Sci.* **377**, 963 (1997).

¹⁰T. G. Walker, A. W. Pang, H. Hopster, and S. F. Alvarado, *Phys. Rev. Lett.* **69**, 1121 (1992).

¹¹F. U. Hillebrecht, C. Roth, R. Jungblut, E. Kisker, and A. Bringer, *Europhys. Lett.* **19**, 711 (1992).

¹²Z. Xu, Y. Liu, P. D. Johnson, and B. S. Itchkawitz, *Phys. Rev. B* **52**, 15 393 (1995).

¹³G. Panaccione, F. Sirotti, E. Narducci, and G. Rossi, *Phys. Rev. B* **55**, 389 (1997).

¹⁴P. Fuchs, V. N. Petrov, K. Totland, and M. Landolt, *Phys. Rev. B* **54**, 9304 (1996).

¹⁵D. S. Gemmell, *Rev. Mod. Phys.* **46**, 129 (1974).

¹⁶C. Rau and R. Sizmann, *Phys. Lett.* **43A**, 317 (1973).

¹⁷F. B. Dunning, C. Rau, and G. K. Walters, *Comments Solid State Phys.* **12**, 17 (1986).

¹⁸H. Winter, H. Hagedorn, R. Zimny, H. Nienhaus, and J. Kirschner, *Phys. Rev. Lett.* **62**, 296 (1989).

¹⁹C. Rau, K. Waters, and N. Chen, *Phys. Rev. Lett.* **64**, 1441 (1990); C. Rau and K. Waters, *Nucl. Instrum. Methods Phys. Res. B* **40/41**, 127 (1989).

²⁰R. Pfandzelter, *Phys. Rev. B* **57**, 15 496 (1998).

²¹J. Kirschner, *Polarized Electrons at Surfaces* (Springer, Berlin, 1985).

²²J. Kirschner and K. Koike, *Surf. Sci.* **273**, 147 (1992).

²³J. Unguris, D. T. Pierce, A. Galejs, and R. J. Celotta, *Phys. Rev. Lett.* **49**, 72 (1982).

²⁴H. Hopster, R. Raue, E. Kisker, G. Güntherodt, and M. Campagna, *Phys. Rev. Lett.* **50**, 70 (1983).

²⁵G. Schönhense and H. C. Siegmann, *Ann. Phys. (Leipzig)* **2**, 465 (1993).

²⁶C. Turtur and G. Bayreuther, *Phys. Rev. Lett.* **72**, 1557 (1994).